ESC European Society of Cardiology

Cardiovascular Research (2022) **118**, 1344–1358
doi:10.1093/cvr/cvab163

Arginase II protein regulates Parkin-dependent p32 degradation that contributes to Ca^{2+}-dependent eNOS activation in endothelial cells

Bon-Hyeock Koo [1], Moo-Ho Won[2], Young-Myeong Kim [3], and Sungwoo Ryoo[1,*]

[1]Department of Biological Sciences, Kangwon National University, Kangwondae-gil 1, Chuncheon 24341, Korea; [2]Departments of Neurobiology, Kangwon National University, Kangwondae-gil 1, Chuncheon 24341, Korea; [3]Molecular and Cellular Biochemistry, Kangwon National University, Kangwondae-gil 1, Chuncheon 24341, Korea

Received 1 October 2020; editorial decision 4 May 2021; accepted 6 May 2021; online publish-ahead-of-print 8 May 2021

Aims Arginase II (ArgII) plays a key role in the regulation of Ca^{2+} between the cytosol and mitochondria in a p32-dependent manner. p32 contributes to endothelial nitric oxide synthase (eNOS) activation through the Ca^{2+}/CaMKII/AMPK/p38MAPK/Akt signalling cascade. Therefore, we investigated a novel function of ArgII in the regulation of p32 stability.

Methods and results mRNA levels were measured by quantitative reverse transcription-PCR, and protein levels and activation were confirmed by western blot analysis. Ca^{2+} concentrations were measured by FACS analysis and a vascular tension assay was performed. ArgII bound to p32, and ArgII protein knockdown using siArgII facilitated the ubiquitin-dependent proteasomal degradation of p32. β-lactone, a proteasome inhibitor, inhibited the p32 degradation associated with endothelial dysfunction in a Ca^{2+}-dependent manner. The amino acids Lys154, Lys 180, and Lys220 of the p32 protein were identified as putative ubiquitination sites. When these sites were mutated, p32 was resistant to degradation in the presence of siArgII, and endothelial function was impaired. Knockdown of Pink/Parkin as an E3-ubiquitin ligase with siRNAs resulted in increased p32, decreased $[Ca^{2+}]c$, and attenuated CaMKII-dependent eNOS activation by siArgII. siArgII-dependent Parkin activation was attenuated by KN93, a CaMKII inhibitor. Knockdown of ArgII mRNA and its gene, but not inhibition of its activity, accelerated the interaction between p32 and Parkin and reduced p32 levels. In aortas of $ArgII^{-/-}$ mice, p32 levels were reduced by activated Parkin and inhibition of CaMKII attenuated Parkin-dependent p32 lysis. siParkin blunted the phosphorylation of the activated CaMKII/AMPK/p38MAPK/Akt/eNOS signalling cascade. However, $ApoE^{-/-}$ mice fed a high-cholesterol diet had greater ArgII activity, significantly attenuated phosphorylation of Parkin, and increased p32 levels. Incubation with siArgII augmented p32 ubiquitination through Parkin activation, and induced signalling cascade activation.

Conclusion The results suggest a novel function for ArgII protein in Parkin-dependent ubiquitination of p32 that is associated with Ca^{2+}-mediated eNOS activation in endothelial cells.

*Corresponding author. Tel: +82 33 250 8534; fax: +82 33 251 3990, E-mail: ryoosw08@kangwon.ac.kr

Graphical Abstract

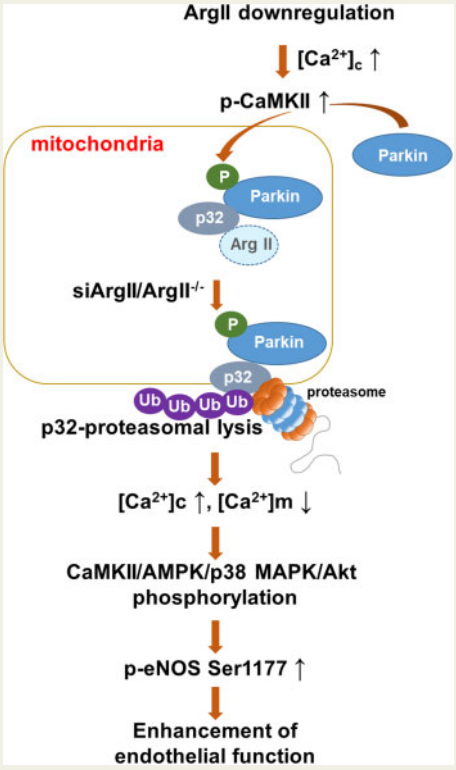

Keywords Arginase II • Parkin • Ubiquitination • p32 • Ca2+ • eNOS • Nitric oxide • Endothelial cells

1. Introduction

Arginase is important for ammonia detoxification, acting in the final reaction of the urea cycle to catalyze the lysis of L-arginine (L-Arg) to L-ornithine and urea. The production of L-ornithine, a polyamine-synthesis precursor, is important for inducing cell proliferation and differentiation.[1,2] Arginase II (ArgII), the extrahepatic isoform, is localized to mitochondria and is the major isoform expressed in aortic endothelial cells (ECs) in both humans and mice. Hypoxia, lipopolysaccharides, and tumour necrosis factor-α induce ArgII expression.[3–5] Upregulated ArgII activity has been demonstrated in blood vessel disorders related to ageing,[6] ischaemia/reperfusion,[7,8] hypertension,[9,10] balloon injury,[11] and atherosclerosis.[12] This upregulation may also contribute to decreased nitric oxide (NO) bioavailability.[6,12,13] In the reciprocally regulated mechanism of ArgII-dependent NO production, ArgII translocation to the cytosol causes a reduction in L-Arg concentration and endothelial NO synthase (eNOS) inactivation. This has been demonstrated in studies with L-Arg as the common substrate for both ArgII and eNOS.[14] We previously reported that ArgII regulates p32-dependent Ca^{2+} translocation from the cytosol to mitochondria by two distinct mechanisms.[13] First, ArgII downregulation decreased the level of spermine, which can bind to p32 and enhance Ca^{2+} movement from the cytosol to mitochondria. Second, reducing the amount of ArgII protein (either via ArgII gene knockout or ArgII siRNA), resulted in reduced levels of p32 protein and increased cytosolic concentrations of Ca^{2+} ($[Ca^{2+}]c$).[13] We therefore suggested the following novel mechanism: ArgII regulates Ca^{2+}-dependent eNOS activity that is also dependent on p32. Accordingly, ArgII-dependent Ca^{2+} regulation via p32 participates in the activation of the signalling cascade, CaMKII/AMPK/p38 MAPK/Akt/eNOS Ser1177 phosphorylation.[15] However, a mechanism linking ArgII protein and p32 stability has not, to our knowledge, been investigated.

The p32 protein, also known as hyaluronan-binding protein 1 (HABP1), is exclusively restricted to mitochondria.[16] However, it is also present on cell membranes as a receptor for both globular head domains complement 1q (gC1qR) and complement 1q-binding protein (C1qbp).[17] This is primarily demonstrated as an SF2 (pre-mRNA splicing factor)-binding protein in the nucleus.[18] In functional studies, p32 plays an essential role in mitochondria-mediated cell death.[19,20] Furthermore, p32 knockdown has been shown to induce less tumorigenic conditions by shifting from an oxidative phosphorylation towards aerobic glycolysis.[21] p32 has also been shown to be involved in morphological changes for both mitochondria and the endoplasmic reticulum. It may influence cellular metabolism and stress responses,[22] and affect the maturation of dendrites by the positive regulation of pyruvate dehydrogenase activity.[23] To date, a number of potential p32-binding partners have been identified. For example, interactions between Parkin and p32 control mitochondrial dynamics and morphology by promoting autophagy-dependent Parkin degradation. However, p32 has been shown not to be a substrate of Parkin in p32-myc-transfected SHSY5Y cells.[22] We have

shown that p32 is crucial in the Ca^{2+}-dependent activation of eNOS in ArgII-downregulated ECs. This led us to suggest p32 as a therapeutic target against endothelial dysfunction-associated vascular diseases.[13]

NO from eNOS is important for the maintenance of vascular homeostasis primarily by modulating vascular tone, but also for the proliferation and migration of vascular smooth muscle cells. Although eNOS activity can be regulated by a variety of factors (e.g. its subcellular localization, extracellular signals, protein–protein interactions, and substrate/cofactor availabilities), $[Ca^{2+}]c$ is also an important contributor to eNOS activity. The activation of calmodulin (Ca^{2+}/CaM) by increased $[Ca^{2+}]c$ promotes the alignment of the reductase and oxygenase domains, and prevents the phosphorylation of eNOS Thr495 through direct binding to the CaM-binding domain in eNOS. Ca^{2+}/CaM also induces Ca^{2+}/CaM-dependent protein kinase II (CaMKII) activation, which phosphorylates eNOS Ser1177 to enhance NO production.[24,25] We believe that understanding the stability of p32 as a regulator of Ca^{2+} translocation between mitochondria and the cytosol will advance the understanding of vascular homeostasis. This led us to identify ArgII as a novel binding partner for p32. Furthermore, we observed that knockdown of the ArgII protein, but not its activity, induced Parkin-dependent proteasomal degradation of p32. Despite the downregulation of ArgII, knockdown of Parkin attenuated Ca^{2+}-mediated eNOS phosphorylation at Ser1177 in a p32-dependent manner, and the translocation of Parkin to mitochondria was dependent on activated CaMKII caused by ArgII downregulation. A role for ArgII protein in Parkin-dependent p32 degradation was also supported by two animal model studies: ArgII gene knockout ($ArgII^{-/-}$) mice and ApoE-null ($ApoE^{-/-}$) mice fed a high-cholesterol diet (HCD) demonstrated increased ArgII activity.

2. Methods

2.1 Materials

We purchased 2(S)-amino-6-boronohexanoic acid (ABH, Cat. No. 194656-75-2) and 2-[N-(2-hydroxyethyl)]-N-(4-methoxybenzenesulfonyl)]amino-N-(4-chlorocinnamyl)-N-methylbenzylamine (KN-93; Cat. No. 422711-1MGCN) from Calbiochem Corp. (La Jolla, CA, USA). Carbobenzoxy-Leu-Leu-Leucinal (MG132, Cat No. 1211877-36-9), clasto-lactacystin β-lactone (β-lactone, Cat. No. 154226-60-5), and chloroquine diphosphate salt (CQ, Cat. No. 50-63-5) were purchased from Sigma-Aldrich (St. Louis, MO, USA). Antisera against eNOS (Cat. No. 610297) and phospho-eNOS (Ser1177, Cat. No. 612392 and Thr495, Cat. No. 612707) were acquired from BD Biosciences (San Jose, CA, USA). Antisera against p32 (Cat. No. ab24733) and Parkin (Cat. No. ab15494) were obtained from Abcam (Cambridge, MA, USA). Akt (also called protein kinase B, Cat. No. #9272), phospho-Akt (Ser473, Cat. No. #9271 and Thr308, Cat. No. #9275), CaMKII (Cat. No. #3362), phospho-CaMKII (Thr286, Cat. No. #12716), AMPK (Cat. No. #2532), phospho-AMPK (Thr172, Cat. No. #2535), and pan-actin (Cat. No. #4968) antisera were purchased from Cell Signaling Technology (Beverly, MA, USA). Phosphoserine (Cat. No. AB1603) antiserum was purchased from Millipore Sigma (Burlington, MA, USA). PTEN-induced Kinase 1 (PINK1, Cat. No. #PA5-13402) and ubiquitin (Cat. No. #13-1600) antibodies were purchased from Invitrogen (Carlsbad, CA, USA). Antisera against Flag (Cat. No. sc-807), ArgII (Cat. No. sc-271443), and heat shock protein 60 (HSP60, Cat. No. sc-13115) were purchased from Santa Cruz Biotechnology (Dallas, TX, USA).

2.2 Cell culture and animals

Human umbilical vein endothelial cells (HUVECs) were purchased from Cascade Biologics (Cat. No. C0035C, Portland, OR, USA) and were maintained according to the supplier's instructions. Ten-week-old male C57BL/6J wild-type (WT) and male $ApoE^{-/-}$ mice (Daehan Biolink Co., Korea) were fed a normal diet (ND, Cat. No. 38057133-27, Nara Biotech. Co., Korea) or a HCD (Cat. No. D12108C, Research Diets, New Brunswick, NJ, USA) for 8 weeks. ECs were isolated from the aorta of anaesthetized mice (100 mg/kg ketamine and 10 mg/kg xylazine, once intraperitoneal injection) as described previously.[12] The $ArgII^{-/-}$ and $p32^{flox/flox}$ $Tie2\text{-}Cre^{+}$ ($p32^{-/-}$) mice were generous gifts from Professors Jaye P.F. Chin-Dusting and Kazuhito Goto, respectively. $ArgII^{-/-}$ mice on a C57BL/6J background, and $p32^{-/-}$ mice on a C57BL/6 background, were maintained at the Kangwon National University Animal Services Facility using a 12-h dark-12-h light cycle and had free access to both food and water. The housing temperature and humidity were 24.2 ± 1.5°C and 51.2 ± 3.9% (mean ± SD), respectively. These studies were performed in accordance with the Guide for the Care and Use of Laboratory Animals (Institutional Review Board, Kangwon National University, KW-17229-2) and were performed in accordance with the US National Institute of Health (NIH) Guide for the Care and Use of Laboratory Animals (NIH Publication, 8th edition). Mice were euthanized with CO_2 at the end of the experiments.

2.3 Quantitative reverse transcription-PCR analysis

Total RNA was extracted using TRIzol reagent (Cat. No. 15596026, Thermo Fisher Scientific, Waltham, MA, USA), and precipitated with isopropyl alcohol. The RNA pellet was washed with 75% ethanol and then dissolved in diethyl pyrocarbonate-treated distilled water. Extracted RNA was equalized among all groups to 2 μg and used to synthesize cDNA (5 min at 37°C, 60 min at 42°C, 10 min at 72°C, 3 min at 4°C) in a thermal cycler (Thermo Fisher Scientific). qPCR was performed with specific primer sets for p32, ArgII, and GAPDH (15 s at 94°C, 30 s at 55°C, 30 s at 72°C for 40 cycles in a real-time quantification thermal cycler; Thermo Fisher Scientific). PCR primers for p32 (Forward: 5′-CTG GCG AGT CTG AAT GGA AGG-3′, Reverse: 5′-GAG CTC CAC CAG CTC ATC TGC-3′), ArgII (Forward: 5′-CUA UCA GCA CUG GAU CUU CUU G-3′, Reverse: 5′-GGG AGU AGG AAG UUG GUC AUA G-3′) were used with GAPDH (Forward: 5′-ACC ACA GTC CAT GCC ATC AC-3′, Reverse: 5′-TCC ACC ACC CTG TTG CTG TA-3′) as a reference.

2.4 Western blot analysis

Western blotting was performed using both cultured cells and aortic tissue. The cells were lysed in SDS sample buffer (62.5 mM Tris–HCl, pH 6.8, 2% SDS, 10% glycerol, 50 mM DTT, 0.01% bromophenol blue). Aortic segments were placed in SDS sample buffer, homogenized 10 times for 2 min each time, and boiled at 100°C for 10 min. The prepared samples from both sources were then centrifuged and used for SDS–polyacrylamide gel electrophoresis. After electrophoresis, the proteins were transferred to polyvinylidene difluoride (PVDF) membranes for 12 h at 4°C (Cat. No. IPVH00010, Millipore). Membranes were blocked with 5% skim milk for 1 h at room temperature, incubated with primary antibody (1:1000) at 4°C for 12 h, and then incubated in horseradish peroxidase-conjugated secondary antibody at room temperature for 2 h. The PVDF chemiluminescence signals were then captured using X-ray film, and band intensities were analysed using NIH ImageJ software (Fiji).

2.5 Co-immunoprecipitation analysis

The cells were washed twice with ice-cold phosphate buffer saline (PBS), lysed with 1x RIPA buffer (Cat No. 20-188, Millipore) containing protease inhibitors (Cat. No. P3100-010, GenDEPOT, Katy, TX, USA), and incubated on ice for 30 min. The lysate was then centrifuged at 15 000 *g* for 15 min at 4°C. The lysate supernatant was pre-cleared by incubating 30 μL of protein A/G bead at 4°C for 6 h (Cat. No. sc-2003, Santa Cruz Biotechnology). After centrifugation at 1000 *g* for 1 min at 4°C, the supernatant was collected and stirred for 24 h at 4°C with 3 μg of IP antibody. Then, the protein A/G bead was incubated for 6 h at 4°C and centrifuged at 1000 *g* for 1 min at 4°C. The supernatant was carefully removed, the protein A/G bead was collected and suspended in PBS and 2x SDS sample buffer, and immunoblotting was performed.

2.6 Measurement of Ca^{2+} concentration $[Ca^{2+}]$ in the cytosol and mitochondrial matrix using flow cytometry

$[Ca^{2+}]$ in the cytosol ($[Ca^{2+}]c$) and mitochondrial matrix ($[Ca^{2+}]m$) were determined using flow cytometry (FACS Calibur, BD Biosciences). The fluorescence intensity of each sample was measured using CellQuest software 5.1 (BD Biosciences). We measured $[Ca^{2+}]c$ over 1 h with 1 μM Fluo-4 AM (Cat. No. F14201, Thermo Fisher Scientific) with an FL1-H-specific fluorescence range, and $[Ca^{2+}]m$ over 1 h with 2 μM Rhod-2 AM (Cat. No. R1244, Thermo Fisher Scientific) with an FL2-H-specific fluorescence range. Changes in $[Ca^{2+}]$ were evaluated by determining fold changes in fluorescence intensities compared to control values.

2.7 Mitochondrial fractionation

Mitochondria were fractionated from HUVECs with 10 mM HEPES buffers (pH 7.6, 1 mM EDTA) having different tonicities: hypotonic, isotonic, and hypertonic conferred by 50 mM, 250 mM, and 450 mM sucrose, respectively. Cells were washed with PBS and homogenized in 100 μL of hypotonic buffer with protease inhibitors, followed by the addition of 100 μL of hypertonic buffer and centrifugation at 1000 *g* for 10 min at 4°C. The supernatant was centrifuged again for 45 min at 21 000 *g* at 4°C. The resulting precipitate was dissolved in isotonic buffer and considered to be the mitochondrial fraction, while the supernatant was considered to be the cytosolic fraction.

2.8 siRNA and p32 plasmid transfection

For transfections of HUVECs with siRNAs, the cells were incubated in starvation medium (DMEM, 5% FBS, and antibiotics) containing an siRNA targeting either Parkin (1989: 5′-UUU ACA GAG AAA CAC CUU GUC AAU G-3′, 2551: 5′-CCG ACU CUC UCC AUC AGA AGG GUU U-3′, Invitrogen), Pink1 (5′-AAG GAU GUU GUC GGA UUU C-3′, Cat. No. D-004030-02-0010, 5′-UUC AUA GGC GAU GGC UCC-3, Cat. No. D-004030-04-0010, Dharmacon, Lafayette, CO), mouse ArgII (siArgII, Cat. No. sc-29729, Santa Cruz Biotechnology), human siArgII (5′-UCU CGA UAG GUU AGU CCC CCG-3′, Bioneer Co., Korea), or scrambled siRNA (scmRNA, Cat. No. sc-37007, Santa Cruz Biotechnology) at 100 nM for 24 h without a reagent. HUVECs were transfected with either 1 μg of the pCMV6-XL5-p32 plasmid (Cat. No. SC107905, OriGene, Rockville, MD, USA), mutated (K154R, K180R, and K220R) p32 plasmid (Macrogen Co., Korea), or the empty plasmid of pCMV6-XL5 using Lipofectamine 3000 (Cat. No. L3000075, Thermo Fisher Scientific). After incubation for 6 h, the cells were cultured for another 24 h in fresh growth medium.

2.9 Preparation of p32-expressing adenovirus

The p32 plasmid, pCMV6-XL5, was purchased from OriGene Co. (Rockville, MD, USA) and subcloned into the *Bgl II*/*Kpn I* restriction sites of the pCMV-Tag1 plasmid. For virus generation, full-length p32 was cloned into the *BamHI* and *XhoI* sites of the pENTR-CMV vector that had attL sites for site-specific recombination with a Gateway destination vector and entry vector (Invitrogen). The site-specific recombination between the pENTR-CMV/p32 and the adenovirus vector, pAd/PL-DEST, was conducted using LR Clonase II. The WT Adp32 is an adenovirus encoding full-length human p32. This adenovirus was amplified in 293A cells and purified using an Adeno-X^{TM} purification kit (Takara, Mountain View, CA, USA) and infection multiplicity was determined using an Adeno-X^{TM} titre kit (Takara). HUVECs were treated with 1×10^6 pfu/mL Adp32. For *in vivo* experiments with mice, we injected 5×10^9 particles of the purified recombinant adenovirus into the tail vein. Adenovirus only (Ad-) was used as a control.

2.10 Measurement of NO

We used 5 μM (final concentration) 4-amino-5-methylamino-2′,7′-difluorofluorescein diacetate (DAF-FM DA; Cat. No. 254109-22-3, Sigma-Aldrich) to measure NO in aortic rings from 10-week-old male WT mice for 5 min with 30 s intervals. Images were acquired using an Olympus BX51 epifluorescence microscope. N^G-nitro-L-arginine methyl ester (L-NAME, Cat. No. 15190-44-0, Sigma-Aldrich) served as the negative control. Fluorescence intensity was measured using Metamorph software 7.6.

2.11 Statistical methods

All experiments were performed using five biological replicates, reported for each experiment. Statistical significance was determined using a one-way ANOVA (mean ± SEM) with Bonferroni *post hoc* tests or using unpaired Student's *t*-tests (mean ± SEM), or using a two-way ANOVA (mean ± SD, GraphPad Prism software 8, GraphPad Inc., San Diego, CA, USA) with Bonferroni correction. *P*-value <0.05 was considered statistically significant.

3. Results

3.1 ArgII protein, as a p32 binding partner, impedes the ubiquitin-dependent proteasomal degradation of p32

A decrease in ArgII protein reduced the amount of mitochondrial p32 protein amount in both siArgII-treated HUVECs and in the aortas of ArgII$^{-/-}$ mice in our previous study.[13] We therefore tested whether siArgII treatment also influenced p32 mRNA levels. As shown in *Figure 1A*, siArgII had no effect on the level p32 mRNA, but siArgII incubation reduced p32 protein levels in a time-dependent manner (*Figure 1B*), increased p32 ubiquitination, and decreased the amount of p32 protein (*Figure 1C*). The proteasome inhibitor MG132 prevented the siArgII-induced degradation of p32 (*Figure 1D*), an effect that we confirmed with β-lactone, another proteasome inhibitor (*Figure 1E*). From the immunoprecipitation analysis, we concluded that ArgII protein was a p32 binding partner in mitochondria (*Figure 1F*). However, ABH, an ArgII inhibitor, had no effect on p32 protein levels (*Figure 1G*). As shown in Supplementary material online, *Figure S1*, we measured $[Ca^{2+}]m$ and $[Ca^{2+}]c$ because p32 accelerated Ca^{2+} movement from the cytosol to

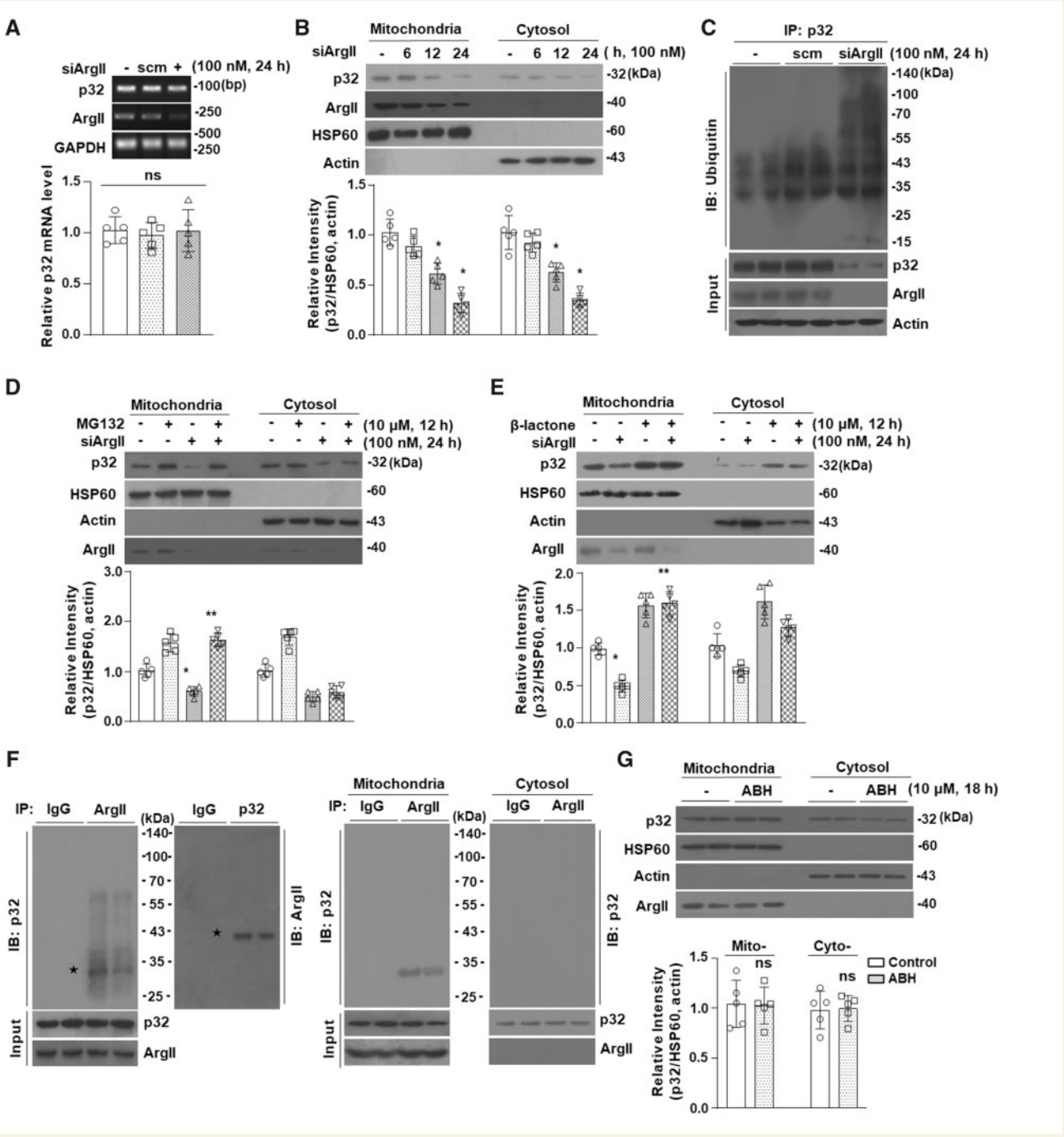

Figure 1 ArgII protein regulates the ubiquitination-dependent proteasomal degradation of p32, and binds to p32 in mitochondria of endothelial cells. (*A*) Quantitative reverse transcription-PCR was performed using p32 and ArgII mRNA after siArgII incubation at 100 nM for 24 h. GAPDH served as the control. (*B*) Western blot analysis of ArgII and p32 proteins in the mitochondria and cytosolic fractions from HUVECs incubated with siArgII at different time points. HSP60 and actin were used as marker proteins for the mitochondrial and cytosolic fractions. *vs. 0 h, $P < 0.0001$ by Student's *t*-test, $P < 0.001$ by one-way ANOVA. (*C*) p32 proteins were immunoprecipitated using an antibody against p32 and immunoblotted using an ubiquitin-detecting antibody after pretreatment with siArgII (100 nM, 24 h). Whole-cell lysates were used as input protein. Representative western blot images from $n = 5$ experiments. (*E*) The preincubation of proteasome inhibitors, MG132 (*D*, 10 μM, 12 h) and clasto-Lactacystin β-lactone (*E*, β-lactone, 10 μM, 12 h) restored mitochondrial p32 level decreased by siArgII treatment. *vs. untreated, $P < 0.001$ by Student's *t*-test; **vs. siArgII, $P < 0.0001$ by Student's *t*-test. (*F*) Immunoprecipitations were performed using antisera against ArgII and p32 and immunoblotted with p32 and ArgII, respectively. Total protein was prepared from cell lysates and the fractionated lysates and their levels were used as inputs. Representative western blot images from $n = 5$ experiments. (*G*) The lysates of HUVECs treated with ABH (10 μM, 18 h) were fractionated and p32 protein in mitochondria was immunoblotted. For all data, $n = 5$ experiments. ns, not significant; scm, scrambled siRNA.

mitochondria and inhibited Ca^{2+}-dependent eNOS activity.[13] siArgII treatment decreased $[Ca^{2+}]m$ and increased $[Ca^{2+}]c$, and these were reversed by incubating with β-lactone and MG132 (Supplementary material online, *Figure S1A and B*). We also noted that β-lactone and MG132 abolished the CaMKII-dependent eNOS activation induced by siArgII treatment through decreased phosphorylation at Ser1177 and increased phosphorylation at Thr495 in HUVECs (Supplementary material online, *Figure S1C*). In the siArgII-treated aortas of WT mice, β-lactone inhibited the siArgII-dependent reduction in p32 levels (Supplementary material online, *Figure S1D*), attenuated acetylcholine (Ach)-dependent vasorelaxation responses (Supplementary material online, *Figure S1E*), and augmented phenylephrine-dependent vasoconstriction (Supplementary material online, *Figure S1F*). However, there were no differences in the responses to KCl (Supplementary material online, *Figure S1G*) or in SNP, an NO donor, responses (Supplementary material online, *Figure S1H*). In addition, β-lactone abolished the siArgII-induced CaMKII/AMPK/Akt/eNOS signalling cascade for eNOS activation (Supplementary material online, *Figure S2*). On the other hand, CQ, a lysosomal inhibitor, had no effect on the decreased p32 levels caused by siArgII treatment (Supplementary material online, *Figure S3*).

3.2 P32 mutations of Lys154, Lys180, and Lys220 to L-Arg enhance p32 stability and attenuate Ca^{2+}-dependent eNOS phosphorylation

We mutagenized (MT) three lysine residues (Lys154, Lys180, and Lys220) to L-Arg in the flag-tagged p32 plasmid encoding p32 cDNA, and confirmed them as putative ubiquitin-binding sites. Transfection of MT p32 plasmid into HUVECs resulted in a decrease in p32 ubiquitination, an increase in p32 protein level (*Figure 2A*), and an increase in p32-bound ArgII protein (*Figure 2B*). Furthermore, transfection of p32 plasmid partially restored the amount of p32 in siArgII-treated HUVECs (*Figure 2C*). p32 overexpression increased the $[Ca^{2+}]m$ that was reduced by siArgII treatment in untransfected and in WT-transfected cells, but the $[Ca^{2+}]m$ in MT-transfected cells was not decreased by siArgII treatment (*Figure 2D*). In contrast, the $[Ca^{2+}]c$ was significantly reduced in both WT- and MT-plasmid-transfected cells overexpressing p32, although siArgII treatment augmented the $[Ca^{2+}]c$ in untransfected and WT-plasmid-transfected cells. The $[Ca^{2+}]c$ was not increased by siArgII in MT p32-expressing cells (*Figure 2E*). These changes of $[Ca^{2+}]c$ influenced CaMKII-dependent eNOS activation. The overexpression of p32 attenuated CaMKII/eNOS Ser1177 phosphorylation, and this was reversed by incubation with siArgII, but MT p32 expression impaired CaMKII-dependent eNOS activation even in the presence of siArgII (*Figure 2F*). Next, we wanted to confirm the stability of both the WT and MT p32 proteins. The WT p32 protein level was decreased by siArgII incubation in a time-dependent manner, but the MT p32 protein amount was not changed by siArgII treatment (Supplementary material online, *Figure S4*). Further tests for the susceptibility of three Lys residues (Lys154, Lys180, and Lys220) in p32 to ubiquitination showed that all three were similarly susceptible to the process (Supplementary material online, *Figure S5*).

3.3 Activated Parkin drives ubiquitin-dependent p32 degradation and mediates eNOS activation through increased $[Ca^{2+}]c$

We next examined which E3-ubiquitin ligase was involved in the ubiquitination of p32 in the absence of ArgII protein. siArgII incubation resulted in Parkin phosphorylation that was blocked by siRNA against Parkin mRNA (siParkin). siParkin treatment only slightly increased the amount of p32 protein, and siArgII-dependent p32 degradation was prevented by siParkin (*Figure 3A*). siArgII treatment induced the movement of Parkin to mitochondria and siPink and siParkin inhibited p32 degradation by siArgII (*Figure 3B*). The ubiquitination of WT p32 protein was markedly reduced in the presence of siParkin, but siParkin had no effect on the ubiquitination of MT p32 protein (*Figure 3C*). As Pink/Parkin regulated p32 stability, we also measured $[Ca^{2+}]m$ and $[Ca^{2+}]c$. Both siPink and siParkin reversed the $[Ca^{2+}]m$ decrease caused by siArgII (*Figure 3D*), and this reversal was accompanied by $[Ca^{2+}]c$ increase (*Figure 3E*). The Ca^{2+}-dependent signalling cascade induced by siArgII (CaMKII/AMPK/Akt/eNOS activation) was attenuated by a siParkin-dependent increase in the amount of p32 protein (*Figure 3F*). Consistent with the western blot analysis, enhanced NO production by siArgII was reduced by siParkin incubation (*Figure 3G*). Unlike our observation with siArgII, the use of ABH, an arginase inhibitor, resulted in both Parkin phosphorylation and its translocation to mitochondria, but, p32 protein levels were not changed (Supplementary material online, *Figure S6*).

3.4 CaMKII-dependent translocation of Parkin to mitochondria regulates p32-dependent Ca^{2+} concentration

Since ArgII downregulation, inhibition, and mRNA knockdown, induced Parkin activation and its translocation, we tested whether activated CaMKII participated in Parkin translocation to mitochondria. The CaMKII inhibitor, KN93, prevented siArgII-mediated Parkin translocation to mitochondria and also increased p32 stability (*Figure 4A*) through reduced p32 ubiquitination (*Figure 4B*). Consistently, CaMKII inhibition prevented the decreases in $[Ca^{2+}]m$ (*Figure 4C*) and increases in $[Ca^{2+}]c$ (*Figure 4D*), caused by siArgII.

3.5 The interaction between p32 and Parkin is physically mediated by ArgII rather than enzymatically

To clarify the function of ArgII protein in Parkin-dependent p32 ubiquitination, we tested for interactions between two proteins, Parkin and p32, under two different conditions: knockdown of ArgII protein using siArgII treatment, and inhibition of ArgII activity with ABH without affecting ArgII protein levels. The decrease in ArgII protein from siArgII treatment enhanced the interaction between p32 and Parkin and reduced the amount of p32 protein. However, ABH neither had an effect on the interaction between p32 and Parkin nor on p32 stability (*Figure 5A*). Likewise, in the aortas of $ArgII^{-/-}$ mice, the interaction of p32 with Parkin was greater and the level of p32 in mitochondria was less compared to those in WT mice (*Figure 5B*). We also investigated the interactions among the three proteins, p32, ArgII, and Parkin. Immunoprecipitation assay showed that Parkin and ArgII precipitated together in both untreated- and scmRNA-treated groups. However, when we treated with sip32, no binding between ArgII and Parkin was detected (Supplementary material online, *Figure S7A and B*). We also confirmed the interactions between ArgII and Parkin in ECs from both WT and $p32^{-/-}$ mice (Supplementary material online, *Figure S7C and D*). In contrast, siParkin treatment had no effect on the interaction between p32 and ArgII proteins (Supplementary material online, *Figure S7E*). From these results, we conclude that ArgII and Parkin proteins are not directly bound to each other, and that p32 is important for their recruitment.

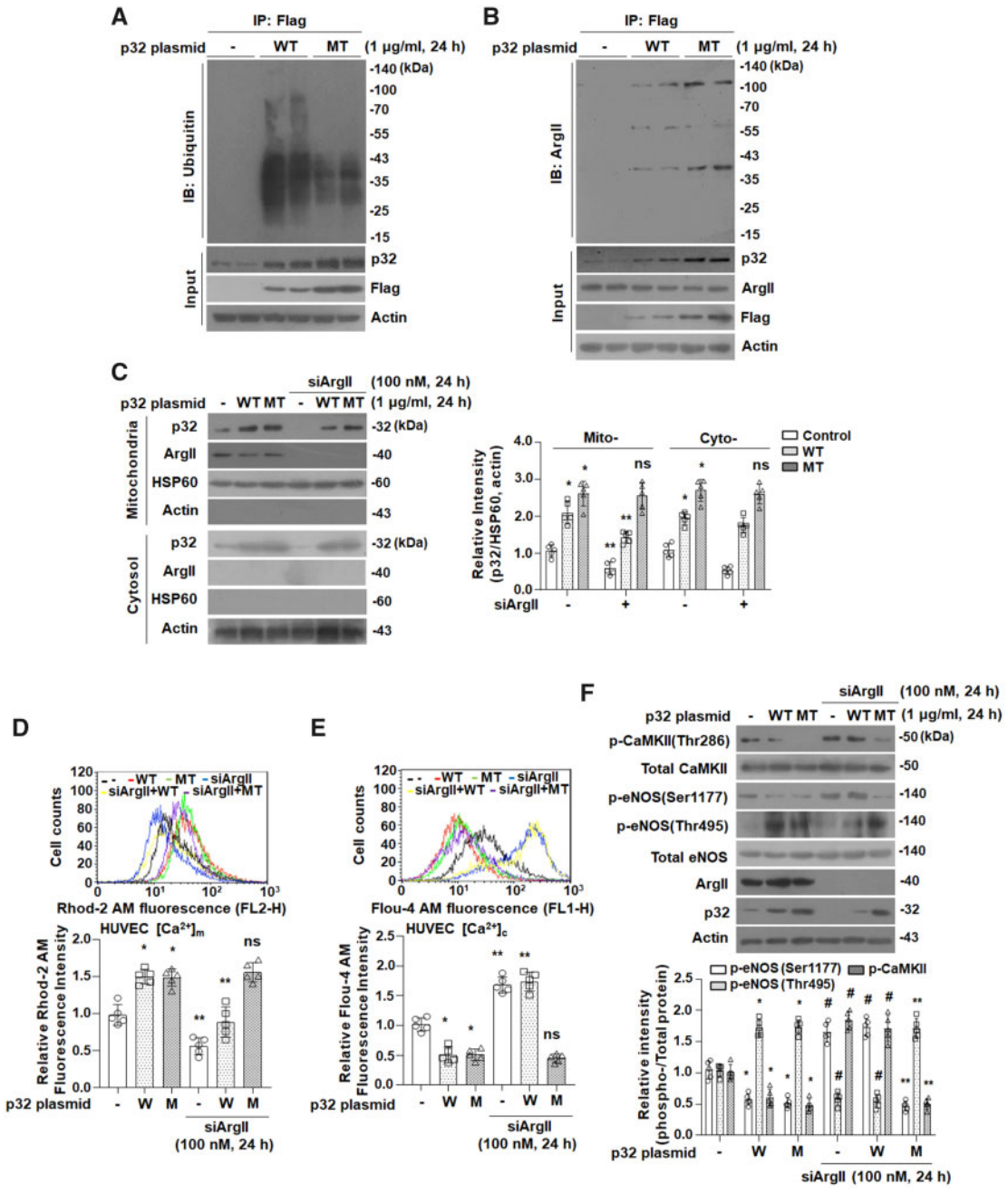

Figure 2 Lys154, Lys180, and Lys220 of p32 are putative ubiquitination sites for ArgII protein knockdown that are involved in Ca^{2+}-dependent eNOS activation. Three Lys residues (Lys154, Lys180, and Lys220) were mutated to L-Arg in a plasmid encoding p32 cDNA, and both flag-tagged WT and mutant (MT) plasmids were transfected into HUVECs. Immunoprecipitations were performed using antisera against the flag. (*A*) Western blotting was performed with anti-ubiquitin antibody. Ubiquitination of flag-tagged p32 was decreased, and the amount of flag-tagged p32 protein was increased in MT-plasmid transfected HUVECs. Representative western blot images from $n = 5$ experiments. (*B*) Western blotting was performed with anti-ArgII antibody. The amount of p32-bound ArgII protein was increased in MT-plasmid transfected HUVECs. Representative western blot images from $n = 5$ experiments. (*C*) Cells lysates were fractionated after the plasmids were transfected and then siArgII was treated. In mitochondrial fractions, siArgII treatment (100 nM, 24 h) decreased p32 protein in both untransfected and WT-plasmid transfected HUVECs. However, p32 protein level was not changed in MT-plasmid transfected HUVECs. In cytosolic fractions, the p32 protein increases due to WT- and MT-plasmid transfections were reduced by siArgII in untransfected and WT-plasmid transfected HUVECs. However, siArgII had no effect on p32 protein level in MT-plasmid transfected HUVECs. *vs. control, $P < 0.0001$ by Student's *t*-test; **vs. untreated (no siArgII), $P < 0.01$ by Student's *t*-test; ns for MT p32-plasmid transfection without siArgII by Student's *t*-test. HUVECs were prepared for FACS analyses after plasmids transfection and siArgII treatment. (*D*) In the analyses for measuring $[Ca^{2+}]$m using Rhod-2 AM, WT- and MT-plasmid transfections increased $[Ca^{2+}]$m, and siArgII reduced $[Ca^{2+}]$m in both untransfected and WT-plasmid transfected HUVECs. However, siArgII had no effect on $[Ca^{2+}]$m in MT-plasmid transfected HUVECs. *vs. untransfected without siArgII, $P < 0.0001$ by Student's *t*-test; **vs. no siArgII, $P < 0.001$ by Student's *t*-test; ns to no siArgII by Student's *t*-test. (*E*) For the $[Ca^{2+}]$c measurements using Fluo-4 AM, WT- and MT-plasmid transfections reduced $[Ca^{2+}]$c, and siArgII increased $[Ca^{2+}]$c in untransfected and WT-plasmid transfected HUVECs. siArgII had no effect on $[Ca^{2+}]$c in MT-plasmid transfected HUVECs. *vs. untransfected

Figure 2 Continued
without siArgII, $P < 0.0001$ by Student's *t*-test; **vs. no siArgII, $P < 0.0001$ by Student's *t*-test; ns for no siArgII by Student's *t*-test. (*F*) HUVECS were transfected with the plasmids and then treated with siArgII. WT- and MT-plasmid transfections decreased CaMKII and eNOS Ser1177 phosphorylation, and increased eNOS Thr495 phosphorylation. Treatment with siArgII augmented CaMKII and eNOS Ser1177 phosphorylation and attenuated eNOS Thr495 phosphorylation in untransfected and WT-plasmid transfected HUVECs. However, MT-plasmid transfection reduced the siArgII effect on CaMKII and eNOS phosphorylation. *vs. untransfected, $P < 0.0001$ by Student's *t*-test; # vs. no siArgII, $P < 0.0001$ by Student's *t*-test; **vs. WT + siArgII, $P < 0.0001$ by Student's *t*-test. For all data, $n = 5$ experiments. ns, not significant.

3.6 Activated Parkin in ArgII$^{-/-}$ mice increases ubiquitin-dependent p32 degradation and eNOS Ser1177 phosphorylation

We next tested whether ArgII protein was involved in Parkin-dependent p32 degradation in aortic tissue from ArgII$^{-/-}$ mice. Parkin phosphorylation at Ser65 was significantly increased, and p32 protein levels were decreased in the aortas of ArgII$^{-/-}$ mice (*Figure 6A*). Phosphorylated Parkin was also translocated to mitochondria in ArgII$^{-/-}$ mice (*Figure 6B*). In ArgII$^{-/-}$ mice, the ubiquitination of p32 was also augmented and accompanied by a decrease in p32 that was restored after siPink and siParkin treatments (*Figure 6C*). A CaMKII inhibitor, KN93, prevented Parkin phosphorylation and increased the p32 amount (*Figure 6D*). In ArgII$^{-/-}$ mice, the enhanced CaMKII/AMPK/Akt/eNOS Ser1177 phosphorylation was attenuated by siParkin incubation (*Figure 6E*). Additionally, β-lactone/MG132 treatments and adenovirus encoding p32 cDNA (adp32) transfection impaired endothelial function through attenuated phosphorylation of CaMKII and eNOS Ser1177 (Supplementary material online, *Figure S8A and B*). Therefore, these results suggest that ArgII downregulation via gene knockout restore endothelial function through Parkin-dependent p32 downregulation, resulting in CaMKII-dependent eNOS activation.

3.7 siArgII restores eNOS Ser1177 phosphorylation through Parkin-mediated p32 ubiquitination in ApoE$^{-/-}$ HCD mice

As ArgII downregulation improved endothelial function in an atherogenic animal model (i.e. ApoE$^{-/-}$ HCD mice), we next examined whether decreased ArgII protein could restore endothelial function through Parkin-dependent p32 downregulation. In the aortas of ApoE$^{-/-}$ HCD mice, Pink and Parkin localization in mitochondria was less, the level of p32 was greater (*Figure 7A*), and Parkin phosphorylation was significantly attenuated (*Figure 7B*). The reduction in p32 ubiquitination was reversed by siArgII incubation (*Figure 7C*), which also reduced the amount of p32 protein (*Figure 7C*), and increased Parkin phosphorylation (*Figure 7D*). The attenuation of CaMKII/AMPK/Akt/eNOS Ser1177 phosphorylation signalling cascade in ApoE$^{-/-}$ + HCD mice was ameliorated by siArgII in a p32-dependent manner that was blocked by siParkin treatment (*Figure 7E*). Therefore, we suggest that p32 regulation is dependent on ArgII protein through a mechanism of Parkin-dependent proteasomal degradation, and this regulation is crucial for endothelial function in ApoE$^{-/-}$ HCD mice.

4. Discussion

The present results have demonstrated that ArgII protein bound to p32 and prevented the ubiquitin-dependent proteasomal degradation of p32; β-lactone and MG132 inhibited p32 lysis, which impaired the endothelial function that was improved by ArgII knockdown; p32 mutations of Lys154, Lys180, and Lys220 enhanced its stability and attenuated Ca^{2+}-dependent eNOS phosphorylation; CaMKII activation (via downregulation of ArgII) induced Parkin phosphorylation, Parkin translocation to mitochondria, and Parkin-mediated ubiquitination of p32; the amount of ArgII protein, not its activity, regulated the interaction between p32 and Parkin; in ArgII$^{-/-}$ mice, activated Parkin accelerated both ubiquitin-dependent p32 degradation and eNOS Ser1177 phosphorylation; and in ApoE$^{-/-}$ + HCD mice, siArgII treatment recovered eNOS Ser1177 phosphorylation through Parkin-mediated p32 degradation.

Previous studies have identified binding partners for p32. The p32 protein has been shown to interact with alpha 1B- and alpha 1D-adrenoreceptors to control their expression and cellular localization,[26] and with PKCμ, which is a regulator of kinase activity and intracellular compartmentalization.[27] The p32 protein has also been shown to interact with nuclear components such as the lamin B receptor, as a linker between the nuclear membrane and intranuclear substructures,[28] and with components of the extracellular matrix, hyaluronic acid,[29] and vitronectin.[30] In addition, p32 interacted with the viral proteins, HIV Tat,[31] and EBV EBNA-1,[32] to augment the transcriptional activation of other viral proteins, and with the bacterial surface protein, InlB, to regulate bacterial invasion into mammalian cells.[17] In addition to these investigations focused on the functional regulation of p32-binding proteins, we suggest a novel ArgII mechanism for Parkin-mediated p32 stability. Although Parkin has been shown to interact with p32,[22] p32 ubiquitination by Parkin has not been demonstrated. As described here, ArgII protein interacted with p32 and prevented Parkin-dependent ubiquitination of p32, and this affected p32 stability. Increased p32 amounts were previously associated with a decrease in $[Ca^{2+}]c$ and impaired Ca^{2+}-dependent eNOS activation.[13] We therefore distinguished the effect of the ArgII protein and its activity on the mechanism of $[Ca^{2+}]c$ regulation. Inhibition of ArgII activity increased $[Ca^{2+}]c$ through a decrease in spermine level, without affecting the amount of p32 protein, and spermine has been identified as a p32-binding molecule that can augment $[Ca^{2+}]m$.[13] Together with the regulation of spermine production, the knockdown of ArgII resulted in increased $[Ca^{2+}]c$ by reducing the amount of p32. Taken together, ArgII is crucial both for the regulation of p32 stability and for p32-dependent Ca^{2+} movement.

Parkin, an E3-ubiquitin ligase, is activated by phosphorylation at Ser65 (*Figure 6A*)[33] and is crucial both for initiating mitophagy and for mitochondrial homeostasis. Parkin mutation has been associated with Parkinson's disease.[34] Its expression in vascular ECs has also been noted,[35] and its activation was reported to have a protective effect on blood vessels in obese, diabetic, and atherosclerotic mice.[36] In addition, the downregulation of ArgII has also been reported to have restored endothelial function in these diseases.[12,37,38] It is well known that Parkin activation can be attributed to activated CaMKII.[36,39] Accordingly, we showed that ArgII downregulation, inhibition of its activity, knockdown

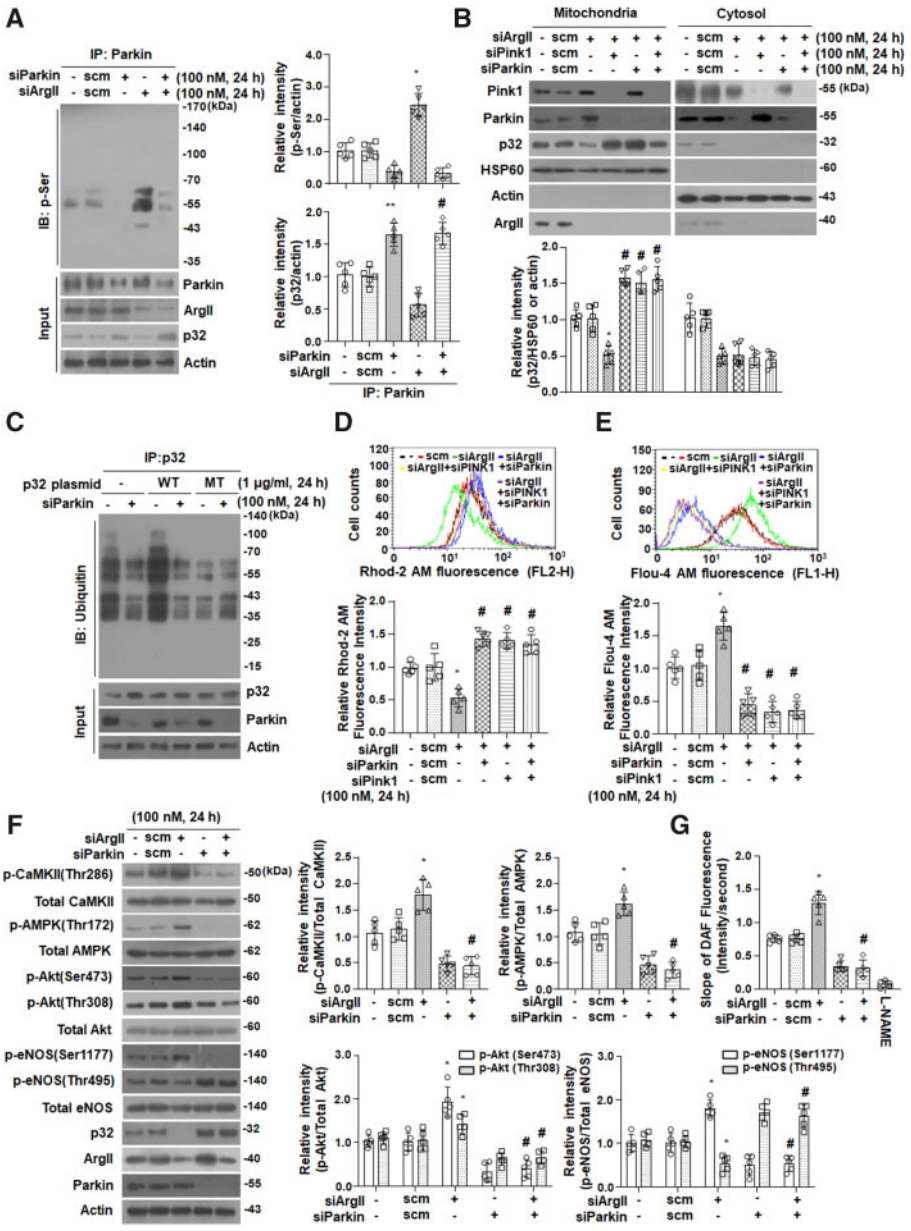

Figure 3 siArgII induces eNOS activation through Pink/Parkin-dependent p32 degradation. (*A*) Parkin was immunoprecipitated, and immunoblotting was performed using anti-phosphoserine antibody in cell lysates from siArgII-treated HUVECs. siArgII treatment (100 nM, 24 h) enhanced Parkin phosphorylation (upper bar graph) and p32 protein was increased by siParkin treatment (lower bar graph). *vs. scm, $P < 0.0001$ by Student's *t*-test; **vs. scm, $P = 0.0001$ by Student's *t*-test; #vs. siArgII, $P < 0.0001$ by Student's *t*-test. (*B*) The lysates of cells treated with siArgII were fractionated. siArgII incubation caused Pink/Parkin translocation to mitochondria and a reduction in p32 protein. Both siPink and siParkin prevented the siArgII-dependent degradation of p32 in mitochondrial fraction. *vs. scm, $P = 0.0004$ by Student's *t*-test; #vs. siArgII, $P < 0.0001$ by Student's *t*-test. (*C*) HUVECs were transfected with either WT- or MT-plasmids and incubated with siParkin for 24 h. p32 ubiquitination was attenuated by siParkin in both untreated and WT-plasmid transfected HUVECs. However, p32 ubiquitination was not changed in MT-plasmid transfected HUVECs. Representative western blot images from $n = 5$ experiments. (*D*) In the FACS analyses to measure $[Ca^{2+}]m$, decreased $[Ca^{2+}]m$ caused by siArgII treatment was reversed by incubation with both siParkin and siPink. *vs. scm, $P = 0.0005$ by Student's *t*-test; #vs. siArgII, $P < 0.0001$ by Student's *t*-test. (*E*) In the measurement of $[Ca^{2+}]c$, increased $[Ca^{2+}]c$ caused by siArgII was reduced by both siParkin and siPink. *vs. scm, $P = 0.0001$ by Student's *t*-test; #vs. siArgII, $P < 0.0001$ by Student's *t*-test. (*F*) In western blotting analyses, siParkin incubation reduced the phosphorylation of CaMKII/AMPK/Akt/eNOS Ser1177 evoked by siArgII. *vs. scm, $P < 0.0001$ by Student's *t*-test; #vs. siArgII, $P < 0.0001$ by Student's *t*-test. For all data, $n = 5$ experiments. (*G*) In aortic endothelia of WT mice, increased NO production by siArgII was blocked by siParkin. *vs. untreated, $P < 0.0001$ by Student's *t*-test; #vs. siArgII, $P < 0.0001$ by Student's *t*-test. $n = 6$ aortic rings from three mice.

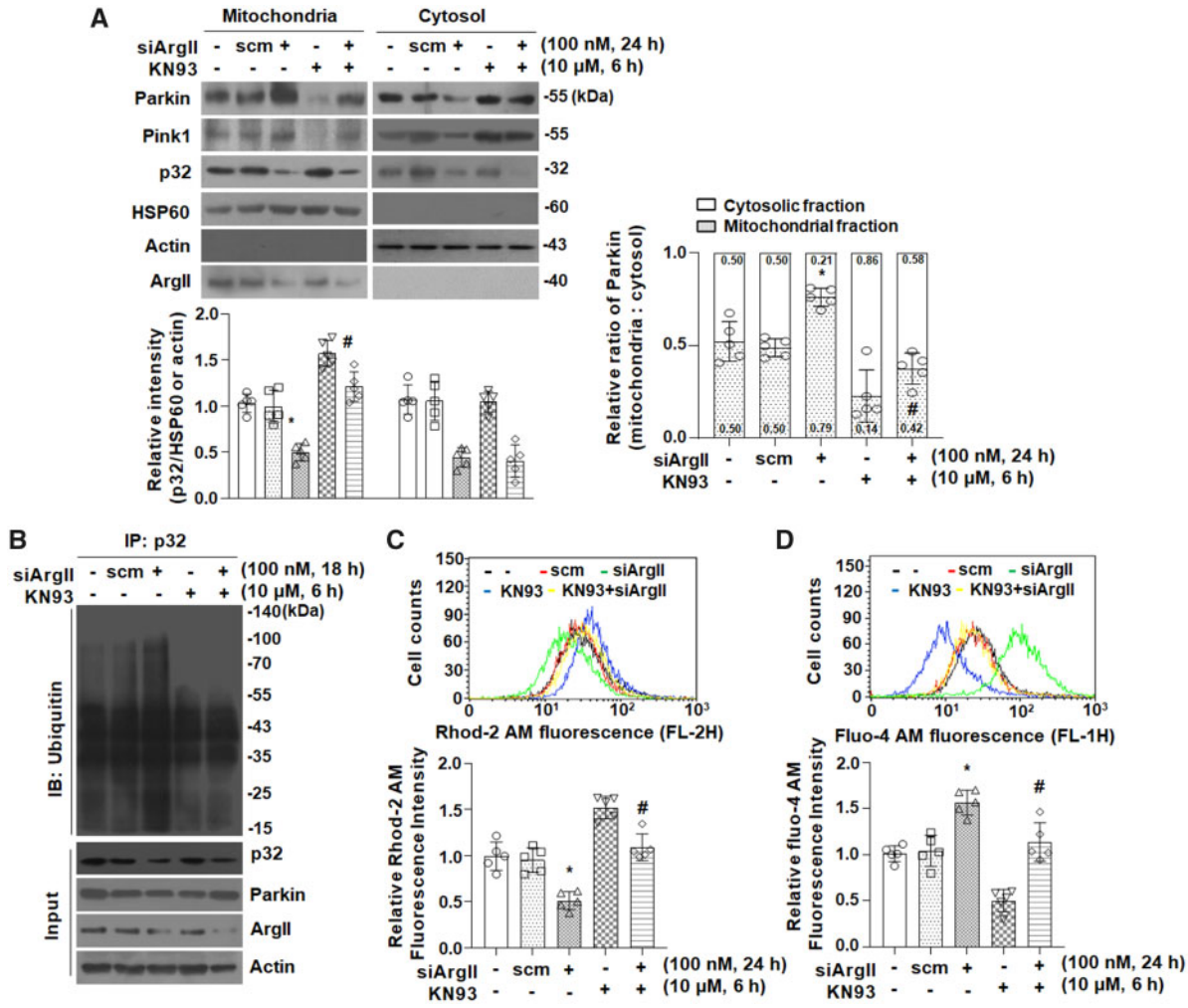

Figure 4 CaMKII, activated by siArgII treatment, elicited Parkin translocation to mitochondria. HUVECs were treated with siArgII and CaMKII inhibitor, KN93. (*A*) siArgII treatment resulted in Pink/Parkin translocation to mitochondria and a reduction in p32 protein that were reversed with KN93. *vs. scm, $P < 0.0001$ by Student's *t*-test; #vs. siArgII, $P < 0.001$ by Student's *t*-test. (*B*) p32 protein was immunoprecipitated and immunoblotted using anti-ubiquitin antibody. Increased p32 ubiquitination by siArgII was decreased by KN93. Representative western blot images from $n = 5$ experiments. (*C*) Reduced $[Ca^{2+}]$m by siArgII was reversed by KN93. *vs. scm, $P = 0.0001$ by Student's *t*-test; #vs. siArgII, $P < 0.0001$ by Student's *t*-test. (*D*) Increased $[Ca^{2+}]$c by siArgII was prevented by KN93. *vs. scm, $P < 0.0001$ by Student's *t*-test; #vs. siArgII, $P = 0.0018$ by Student's *t*-test. For all data, $n = 5$ experiments.

of the protein, and gene knockout, induced the phosphorylation and translocation of Parkin to mitochondria through the activation of CaMKII by increased $[Ca^{2+}]$c. In contrast, increased ArgII activity in ApoE$^{-/-}$ + HCD mice showed attenuated Parkin activation and endothelial dysfunction, which was reversed by siArgII treatment (*Figure 7*). This result was attributed to the HCD because oxidized low-density lipoprotein has been shown to increase the amount of p32.[13] Thus, ArgII protein may be a useful tool for the development of a novel strategy to elicit Parkin activation.

We observed that p32 may be ubiquitinated at three lysine residues (Lys154, Lys180, and Lys220); this was demonstrated using the UbPred prediction software (http://www.ubpred.org/). When these amino acids were mutated to L-Arg, ubiquitination of p32 was reduced (*Figure 3*). Although we did not determine that each individual Lys residue was susceptible to ubiquitination, we demonstrated that the three were related to ubiquitination and p32 stability (Supplementary material online, *Figures S4 and S5*). Predicted by the PyMOL software program, p32 protein could interact with ArgII and Parkin (Supplementary material online, *Figure S7F and G*), and the common binding site was located from Lys179 to Tyr188 of p32. This result is consistent with our experimental data (*Figure 5* and Supplementary material online, *Figure S5*). Taken together, we can schematically describe the interaction of p32, ArgII, and Parkin (*Figure 8*). ArgII downregulation, ABH, and siArgII, increased $[Ca^{2+}]$c and then induced CaMKII-dependent Parkin activation. However, ABH inhibited enzyme activity without affecting the amount of ArgII protein. The interaction between ArgII and p32 was not changed in the presence of ABH, and ArgII bound to the p32 ubiquitination sites (Lys154, Lys180, and Lys220) and prevented Parkin-dependent p32 ubiquitination through steric hindrance. In contrast, siArgII treatment decreased ArgII protein amount and exposed the p32 ubiquitination sites that increased Parkin-dependent degradation of p32.

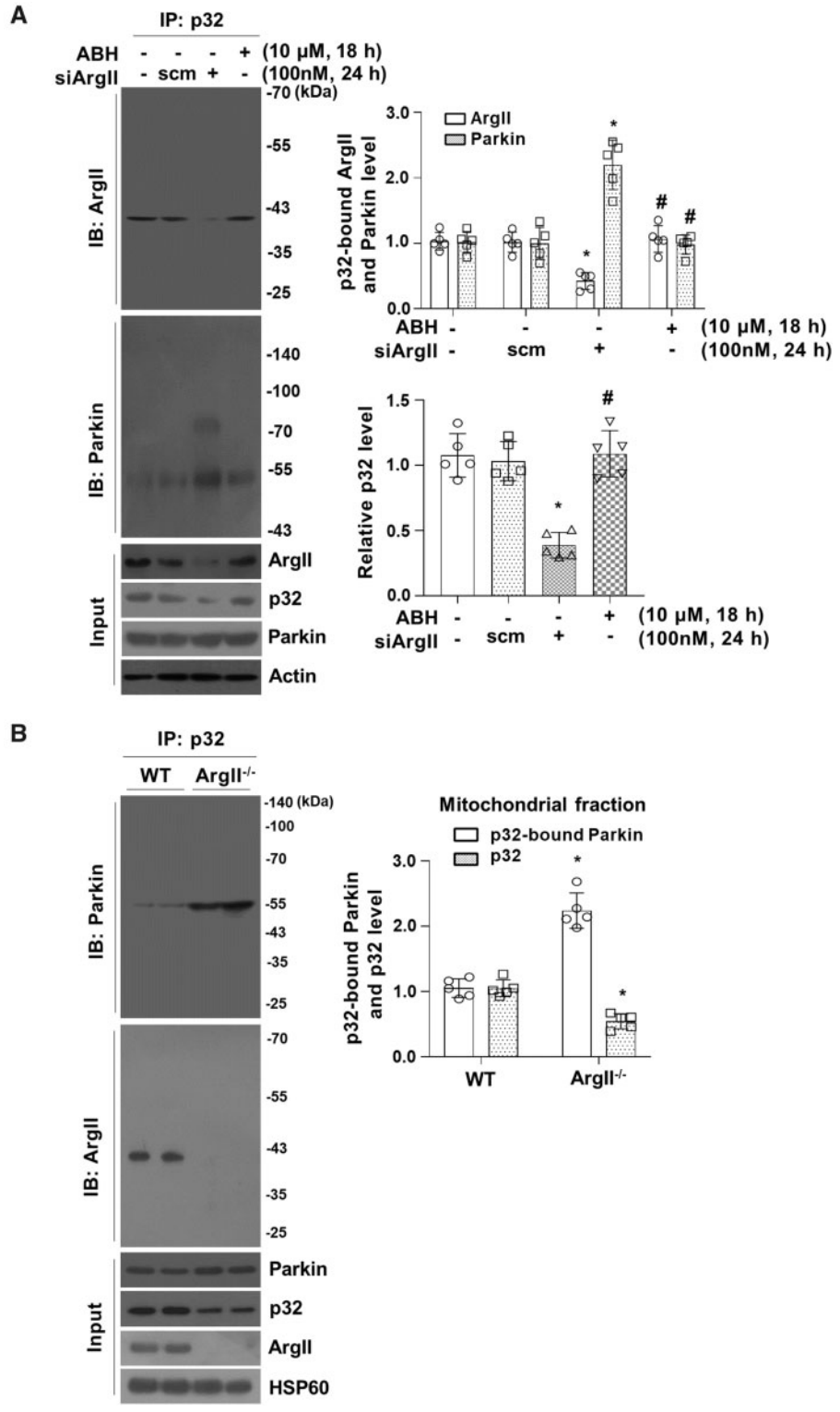

Figure 5 Knockdown of ArgII protein, not inhibiting its activity, enhanced p32-Parkin binding. (*A*) The lysates from siArgII- and ABH-treated HUVECs were immunoprecipitated using p32 antibody and immunoblotted using ArgII and Parkin antibodies. siArgII treatment resulted in an increase in the amount of p32-interacted Parkin, although the amount of p32 protein decreased. *vs. scm, $P < 0.0001$ by Student's *t*-test; #vs. untreated, ns by Student's *t*-test. (*B*) Mitochondria fractions were obtained from aortic tissue from WT and ArgII$^{-/-}$ mice, and p32 protein was immunoprecipitated. p32-bound Parkin amount was high, but p32 amount was low in ArgII$^{-/-}$ mice. *vs. WT, $P < 0.001$ by Student's *t*-test. For all data, $n = 5$ experiments. ns, not significant.

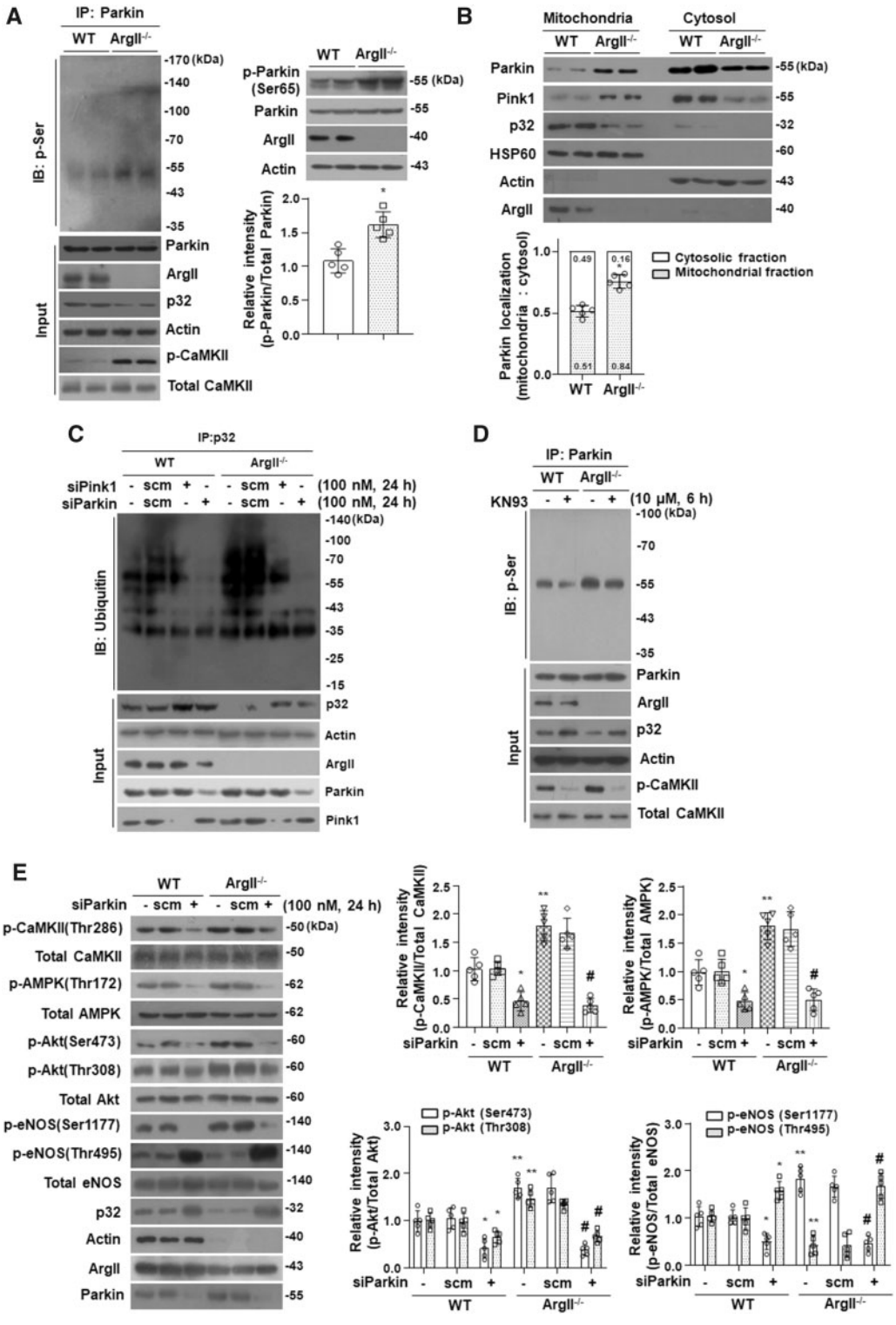

Figure 6 Activated Pink/Parkin negatively regulates p32 stability that activates eNOS in the aortas of ArgII$^{-/-}$ mice. (*A*) Parkin phosphorylation was assessed by immunoprecipitation and western blotting with anti-phosphoserine and phospho-Parkin Ser65 antibodies, respectively. In aortic vessels of ArgII$^{-/-}$, p32 protein level decreased, and Parkin phosphorylation at Ser65 increased. *vs. WT, $P = 0.0019$ by Student's *t*-test. Representative western blot images from $n = 5$ experiments. (*B*) Aortic lysates were fractionated into mitochondria and cytosol. Pink/Parkin was localized in mitochondria in ArgII$^{-/-}$ mice. *vs. WT, $P < 0.0001$ by Student's *t*-test. (*C*) SiPink and siParkin were incubated with aortas and p32 was immunoprecipitated. p32 ubiquitination was enhanced, and siPink and siParkin reduced p32 ubiquitination in ArgII$^{-/-}$ mice. Representative western blot images from $n = 5$ experiments. (*D*) In ArgII$^{-/-}$ mice, KN93 attenuated Parkin phosphorylation and restored p32 protein amount. Representative western blot images from $n = 5$ experiments. (*E*) Isolated aortas from WT and ArgII$^{-/-}$ mice were incubated with siParkin. siParkin blunted increased CaMKII/AMPK/Akt/eNOS Ser1177 phosphorylation in aortas of ArgII$^{-/-}$ mice. *vs. untreated (WT), $P < 0.001$ by Student's *t*-test, **vs. untreated (WT), $P < 0.001$ by Student's *t*-test, $^{\#}$vs. untreated (ArgII$^{-/-}$), $P < 0.0001$ by Student's *t*-test. For all data, $n = 5$ experiments.

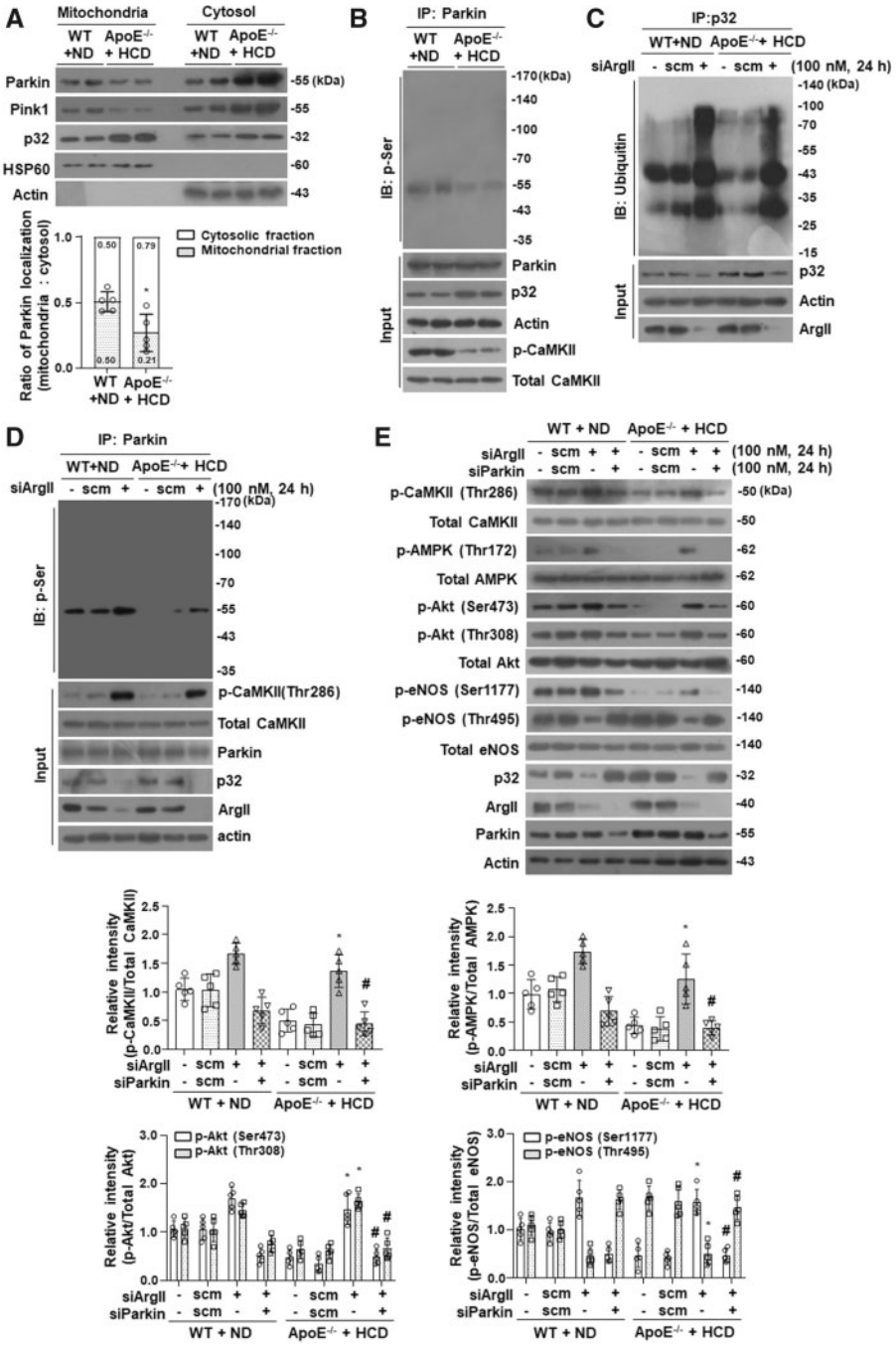

Figure 7 siArgII increases Parkin-dependent ubiquitination of p32 that activates eNOS in aortas of ApoE$^{-/-}$ HCD mice. Aortic lysates from ApoE$^{-/-}$ HCD and WT ND mice were fractionated. (*A*) In mitochondria, Pink/Parkin proteins were reduced and p32 protein was increased in aortas of ApoE$^{-/-}$ HCD mice. *vs. WT ND, $P < 0.001$ by Student's *t*-test. (*B*) In immunoprecipitation experiments, Parkin phosphorylation was reduced in ApoE$^{-/-}$ HCD mice. Representative western blot images from $n = 5$ experiments. (*C*) p32 ubiquitination was decreased and siArgII enhanced p32 ubiquitination. Representative western blot images from $n = 5$ experiments. (*D*) siArgII increased Parkin phosphorylation and reduced p32 protein amount. Representative western blot images from $n = 5$ experiments. (*E*) Immunoblotting was performed with aortas treated with siArgII and siParkin. In aortas of ApoE$^{-/-}$ HCD mice, siArgII restored the CaMKII/AMPK/Akt/eNOS Ser1177 phosphorylations that were attenuated by siParkin. *vs. untreated (ApoE$^{-/-}$ HCD), $P < 0.001$ by Student's *t*-test, # vs. siArgII (ApoE$^{-/-}$ HCD), $P < 0.0001$ by Student's *t*-test. For all data, $n = 5$ experiments.

The conserved eukaryotic p32 protein is both multifunctional and multicompartmental (targeted to different organelles). A functional p32 study using heterozygous mice fed a high-fat diet (HFD) reported lower body weights, fat, and blood glucose levels, but higher fatty acid oxidation/glycolysis, energy expenditure, and resistance to hepatosteatosis.[40] In addition, the partial suppression of p32 reduced lipid accumulation through downregulation of lipogenic genes such as *srebp1*, *Fasn*, and *Acc*.[41] Moreover, severe disruption to the mitochondrial respiratory

chain has been reported in p32$^{-/-}$ embryos.[42] Interestingly, the metabolic properties of p32 heterozygous HFD mice were similar to those of ArgII$^{-/-}$ mice fed a high-fat high-sucrose diet.[37] The ArgII$^{-/-}$ mice had lower blood glucose levels, higher energy expenditures, upregulated genes associated with fatty acid oxidation, and activated AMPK. Another ArgII$^{-/-}$ HFD mouse study showed lower hepatic steatosis, lower levels of a lipogenic transcription factor, SREBP-1c, lower activity/expression of lipogenic enzymes, and higher AMPK activation.[38] These studies revealed the same metabolic shift in both p32 heterozygous and ArgII$^{-/-}$ mice, which is consistent with changes in mitochondrial Ca^{2+} levels. Mitochondrial Ca^{2+} influx serves as a rapid signal for the allosteric activation of select matrix dehydrogenases of the tricarboxylic acid cycle, as well as for mitochondrial ATP synthase, to collectively enhance energy output.[43,44] In our previous study, we reported that ArgII downregulation and p32 knockdown with siRNA resulted in CaMKII-dependent AMPK activation through increased [Ca^{2+}]c.[15] Lower [Ca^{2+}]m inhibits mitochondrial respiration (= reduced glucose oxidation), shifts it towards fatty acid metabolism, and reduces body fat.[45] Consistent with this demonstration, abrogation of mitochondrial Ca^{2+} influx disrupts oxidative phosphorylation and AMPK activation.[46] Therefore, our finding that ArgII protein regulated [Ca^{2+}]m through Parkin-dependent ubiquitination of p32 protein may explain the metabolic similarities between the two mice models. In addition, the present study may contribute to the understanding of diseases such as Parkinson's and Alzheimer's, which are characterized by perturbations in Ca^{2+} homeostasis and mitochondrial dysfunction.[47] With this in mind, we also examined mitochondrial function (Supplementary material online, *Figure S9*). Mitochondrial content was not different among the three groups (WT, ArgII$^{-/-}$, and p32$^{f/f}$ Tie-Cre^{+}). Mitochondrial fragmentation was increased, and ATP levels decreased, in ArgII$^{-/-}$ and p32$^{f/f}$ Tie-Cre^{+} mice compared to WT. Additionally, mitochondrial membrane potential was decreased in the p32$^{f/f}$ Tie-Cre^{+} group. The protein levels, MFN2 and DRP1, associated with mitochondrial fusion and fission were not different, but the levels of LC3-II, which was associated with autophagy, were higher in the ArgII$^{-/-}$ group.

The ArgII enzyme catalyzes L-Arg to L-ornithine and urea, an important step both in the urea cycle and in the regulation of L-Arg bioavailability. The latter may contribute to eNOS activation through increased substrate accessibility.[6] Moreover, we have reported that ArgII protein and its activity participate in the Ca^{2+} flux between mitochondria and the cytosol in a p32-dependent manner.[13,48] Here, we propose two novel functions for ArgII: First, that ArgII regulates CaMKII-dependent Parkin activation and its translocation to mitochondria (*Figure 4*); and second, that ArgII protein negatively regulates Parkin-dependent p32 ubiquitination (*Figure 8*). However, we did not determine the mechanism by which ArgII downregulation increased [Ca^{2+}]c, although p32 knockdown did increase [Ca^{2+}]c. We conclude that Ca^{2+} moved into the cytosol from elsewhere, as p32 facilitated Ca^{2+} movement from the cytosol to mitochondria. We suggest that L-Arg may be associated with increased [Ca^{2+}]c because L-Arg itself increases [Ca^{2+}]c in our previous study.[13] This postulation may be applied to explain the L-Arg paradox.

Supplementary material

Supplementary material is available at *Cardiovascular Research* online.

Conflict of interest: none declared.

Funding

This work was supported by the Basic Science Research Program of the National Research Foundation of Korea funded by the Ministry of Education, Science and Technology (2016M3A9B6903185 and 2018R1D1A1B07047959).

Data availability

The data underlying this article will be shared on reasonable request to the corresponding author.

Acknowledgements

We thank the Central Laboratory of Kangwon National University for technical assistance and Professor Kazuhito Goto for the p32$^{flox/flox}$ Tie2-Cre^{+} mice.

References

1. Ignarro LJ, Buga GM, Wei LH, Bauer PM, Wu G, del Soldato P. Role of the arginine-nitric oxide pathway in the regulation of vascular smooth muscle cell proliferation. *Proc Natl Acad Sci USA* 2001;**98**:4202–4208.
2. Li H, Meininger CJ, Hawker JR Jr, Haynes TE, Kepka-Lenhart D, Mistry SK, Morris SM Jr, Wu G. Regulatory role of arginase I and II in nitric oxide, polyamine, and proline syntheses in endothelial cells. *Am J Physiol Endocrinol Metab* 2001;**280**:E75–E82.
3. Morris SM Jr, Kepka-Lenhart D, Chen LC. Differential regulation of arginases and inducible nitric oxide synthase in murine macrophage cells. *Am J Physiol* 1998;**275**:E740–E747.
4. Louis CA, Reichner JS, Henry WL Jr, Mastrofrancesco B, Gotoh T, Mori M, Albina JE. Distinct arginase isoforms expressed in primary and transformed macrophages: regulation by oxygen tension. *Am J Physiol* 1998;**274**:R775–R782.
5. Collado B, Sanchez-Chapado M, Prieto JC, Carmena MJ. Hypoxia regulation of expression and angiogenic effects of vasoactive intestinal peptide (VIP) and VIP receptors in LNCaP prostate cancer cells. *Mol Cell Endocrinol* 2006;**249**:116–122.
6. Berkowitz DE, White R, Li D, Minhas KM, Cernetich A, Kim S, Burke S, Shoukas AA, Nyhan D, Champion HC, Hare JM. Arginase reciprocally regulates nitric oxide synthase activity and contributes to endothelial dysfunction in aging blood vessels. *Circulation* 2003;**108**:2000–2006.
7. Hein TW, Zhang C, Wang W, Chang CI, Thengchaisri N, Kuo L. Ischemia-reperfusion selectively impairs nitric oxide-mediated dilation in coronary arterioles: counteracting role of arginase. *FASEB J* 2003;**17**:2328–2330.
8. Jung C, Gonon AT, Sjoquist PO, Lundberg JO, Pernow J. Arginase inhibition mediates cardioprotection during ischaemia-reperfusion. *Cardiovasc Res* 2010;**85**:147–154.
9. Johnson FK, Johnson RA, Peyton KJ, Durante W. Arginase inhibition restores arteriolar endothelial function in Dahl rats with salt-induced hypertension. *Am J Physiol Regul Integr Comp Physiol* 2005;**288**:R1057–R1062.
10. Zhang C, Hein TW, Wang W, Miller MW, Fossum TW, McDonald MM, Humphrey JD, Kuo L. Upregulation of vascular arginase in hypertension decreases nitric oxide-mediated dilation of coronary arterioles. *Hypertension* 2004;**44**:935–943.
11. Peyton KJ, Ensenat D, Azam MA, Keswani AN, Kannan S, Liu XM, Wang H, Tulis DA, Durante W. Arginase promotes neointima formation in rat injured carotid arteries. *Arterioscler Thromb Vasc Biol* 2009;**29**:488–494.
12. Ryoo S, Gupta G, Benjo A, Lim HK, Camara A, Sikka G, Lim HK, Sohi J, Santhanam L, Soucy K, Tuday E, Baraban E, Ilies M, Gerstenblith G, Nyhan D, Shoukas A, Christianson DW, Alp NJ, Champion HC, Huso D, Berkowitz DE. Endothelial arginase II: a novel target for the treatment of atherosclerosis. *Circ Res* 2008;**102**:923–932.
13. Koo BH, Hwang HM, Yi BG, Lim HK, Jeon BH, Hoe KL, Kwon YG, Won MH, Kim YM, Berkowitz DE, Ryoo S. Arginase II contributes to the Ca(2+)/CaMKII/eNOS axis by regulating Ca(2+) concentration between the cytosol and mitochondria in a p32-dependent manner. *J Am Heart Assoc* 2018;**7**:e009579.
14. Pandey D, Bhunia A, Oh YJ, Chang F, Bergman Y, Kim JH, Serbo J, Boronina TN, Cole RN, Van Eyk J, Remaley AT, Berkowitz DE, Romer LH. OxLDL triggers retrograde translocation of arginase2 in aortic endothelial cells via ROCK and mitochondrial processing peptidase. *Circ Res* 2014;**115**:450–459.
15. Koo BH, Won MH, Kim YM, Ryoo S. p32-dependent p38 MAPK activation by arginase II downregulation contributes to endothelial nitric oxide synthase activation in HUVECs. *Cells* 2020;**9**:392–407.
16. Ghebrehiwet B, Lim BL, Peerschke EI, Willis AC, Reid KB. Isolation, cDNA cloning, and overexpression of a 33-kD cell surface glycoprotein that binds to the globular "heads" of C1q. *J Exp Med* 1994;**179**:1809–1821.

17. Krainer AR, Mayeda A, Kozak D, Binns G. Functional expression of cloned human splicing factor SF2: homology to RNA-binding proteins, U1 70K, and Drosophila splicing regulators. *Cell* 1991;**66**:383–394.
18. Muta T, Kang D, Kitajima S, Fujiwara T, Hamasaki N. p32 protein, a splicing factor 2-associated protein, is localized in mitochondrial matrix and is functionally important in maintaining oxidative phosphorylation. *J Biol Chem* 1997;**272**:24363–24370.
19. Itahana K, Zhang Y. Mitochondrial p32 is a critical mediator of ARF-induced apoptosis. *Cancer Cell* 2008;**13**:542–553.
20. Sunayama J, Ando Y, Itoh N, Tomiyama A, Sakurada K, Sugiyama A, Kang D, Tashiro F, Gotoh Y, Kuchino Y, Kitanaka C. Physical and functional interaction between BH3-only protein Hrk and mitochondrial pore-forming protein p32. *Cell Death Differ* 2004;**11**:771–781.
21. Fogal V, Richardson AD, Karmali PP, Scheffler IE, Smith JW, Ruoslahti E. Mitochondrial p32 protein is a critical regulator of tumor metabolism via maintenance of oxidative phosphorylation. *Mol Cell Biol* 2010;**30**:1303–1318.
22. Li Y, Wan OW, Xie W, Chung KK. p32 regulates mitochondrial morphology and dynamics through Parkin. *Neuroscience* 2011;**199**:346–358.
23. Gotoh K, Morisaki T, Setoyama D, Sasaki K, Yagi M, Igami K, Mizuguchi S, Uchiumi T, Fukui Y, Kang D. Mitochondrial p32/C1qbp is a critical regulator of dendritic cell metabolism and maturation. *Cell Rep* 2018;**25**:1800–1815.e1804.
24. Fleming I, Fisslthaler B, Dimmeler S, Kemp BE, Busse R. Phosphorylation of Thr(495) regulates Ca(2+)/calmodulin-dependent endothelial nitric oxide synthase activity. *Circ Res* 2001;**88**:E68–E75.
25. Salerno JC, Harris DE, Irizarry K, Patel B, Morales AJ, Smith SM, Martasek P, Roman LJ, Masters BS, Jones CL, Weissman BA, Lane P, Liu Q, Gross SS. An autoinhibitory control element defines calcium-regulated isoforms of nitric oxide synthase. *J Biol Chem* 1997;**272**:29769–29777.
26. Pupo AS, Minneman KP. Specific interactions between gC1qR and alpha1-adrenoceptor subtypes. *J Recept Signal Transduct Res* 2003;**23**:185–195.
27. Storz P, Hausser A, Link G, Dedio J, Ghebrehiwet B, Pfizenmaier K, Johannes FJ. Protein kinase C [micro] is regulated by the multifunctional chaperon protein p32. *J Biol Chem* 2000;**275**:24601–24607.
28. Simos G, Georgatos SD. The lamin B receptor-associated protein p34 shares sequence homology and antigenic determinants with the splicing factor 2-associated protein p32. *FEBS Lett* 1994;**346**:225–228. [CVOCROSSCVO]
29. Deb TB, Datta K. Molecular cloning of human fibroblast hyaluronic acid-binding protein confirms its identity with P-32, a protein co-purified with splicing factor SF2. Hyaluronic acid-binding protein as P-32 protein, co-purified with splicing factor SF2. *J Biol Chem* 1996;**271**:2206–2212.
30. Lim BL, Reid KB, Ghebrehiwet B, Peerschke EI, Leigh LA, Preissner KT. The binding protein for globular heads of complement C1q, gC1qR. Functional expression and characterization as a novel vitronectin binding factor. *J Biol Chem* 1996;**271**:26739–26744.
31. Yu L, Zhang Z, Loewenstein PM, Desai K, Tang Q, Mao D, Symington JS, Green M. Molecular cloning and characterization of a cellular protein that interacts with the human immunodeficiency virus type 1 Tat transactivator and encodes a strong transcriptional activation domain. *J Virol* 1995;**69**:3007–3016.
32. Wang Y, Finan JE, Middeldorp JM, Hayward SD. P32/TAP, a cellular protein that interacts with EBNA-1 of Epstein-Barr virus. *Virology* 1997;**236**:18–29.
33. Kazlauskaite A, Kondapalli C, Gourlay R, Campbell DG, Ritorto MS, Hofmann K, Alessi DR, Knebel A, Trost M, Muqit MM. Parkin is activated by PINK1-dependent phosphorylation of ubiquitin at Ser65. *Biochem J* 2014;**460**:127–139.
34. Dawson TM, Dawson VL. The role of Parkin in familial and sporadic Parkinson's disease. *Mov Disord* 2010;**25(Suppl 1)**: S32–S39.
35. Tamo W, Imaizumi T, Tanji K, Yoshida H, Takanashi S, Wakabayashi K, Takahashi R, Hattori N, Satoh K. Parkin is expressed in vascular endothelial cells. *Neurosci Lett* 2007;**419**:199–201.
36. Li P, Bai Y, Zhao X, Tian T, Tang L, Ru J, An Y, Wang J. NR4A1 contributes to high-fat associated endothelial dysfunction by promoting CaMKII-Parkin-mitophagy pathways. *Cell Stress Chaperones* 2018;**23**:749–761.
37. Atawia RT, Toque HA, Meghil MM, Benson TW, Yiew NKH, Cutler CW, Weintraub NL, Caldwell RB, Caldwell RW. Role of arginase 2 in systemic metabolic activity and adipose tissue fatty acid metabolism in diet-induced obese mice. *Int J Mol Sci* 2019;**20**:1462–1482.
38. Liu C, Rajapakse AG, Riedo E, Fellay B, Bernhard MC, Montani JP, Yang Z, Ming XF. Targeting arginase-II protects mice from high-fat-diet-induced hepatic steatosis through suppression of macrophage inflammation. *Sci Rep* 2016;**6**:20405.
39. Zhao Q, Wang W, Cui J. Melatonin enhances TNF-alpha-mediated cervical cancer HeLa cells death via suppressing CaMKII/Parkin/mitophagy axis. *Cancer Cell Int* 2019;**19**:58.
40. Liu Y, Leslie PL, Jin A, Itahana K, Graves LM, Zhang Y. p32 heterozygosity protects against age- and diet-induced obesity by increasing energy expenditure. *Sci Rep* 2017;**7**:5754.
41. Liu Y, Leslie PL, Jin A, Itahana K, Graves LM, Zhang Y. p32 regulates ER stress and lipid homeostasis by down-regulating GCS1 expression. *FASEB J* 2018;**32**:3892–3902.
42. Yagi M, Uchiumi T, Takazaki S, Okuno B, Nomura M, Yoshida S, Kanki T, Kang D. p32/gC1qR is indispensable for fetal development and mitochondrial translation: importance of its RNA-binding ability. *Nucleic Acids Res* 2012;**40**:9717–9737.
43. Denton RM. Regulation of mitochondrial dehydrogenases by calcium ions. *Biochim Biophys Acta* 2009;**1787**:1309–1316.
44. Jouaville LS, Pinton P, Bastianutto C, Rutter GA, Rizzuto R. Regulation of mitochondrial ATP synthesis by calcium: evidence for a long-term metabolic priming. *Proc Natl Acad Sci USA* 1999;**96**:13807–13812.
45. Kwong JQ, Huo J, Bround MJ, Boyer JG, Schwanekamp JA, Ghazal N, Maxwell JT, Jang YC, Khuchua Z, Shi K, Bers DM, Davis J, Molkentin JD. The mitochondrial calcium uniporter underlies metabolic fuel preference in skeletal muscle. *JCI Insight* 2018;**3**:e121689.
46. Mallilankaraman K, Cardenas C, Doonan PJ, Chandramoorthy HC, Irrinki KM, Golenar T, Csordas G, Madireddi P, Yang J, Muller M, Miller R, Kolesar JE, Molgo J, Kaufman B, Hajnoczky G, Foskett JK, Madesh M. MCUR1 is an essential component of mitochondrial Ca2+ uptake that regulates cellular metabolism. *Nat Cell Biol* 2012;**14**:1336–1343.
47. Pivovarova NB, Andrews SB. Calcium-dependent mitochondrial function and dysfunction in neurons. *FEBS J* 2010;**277**:3622–3636.
48. Koo BH, Hong D, Hong HD, Lim HK, Hoe KL, Won MH, Kim YM, Berkowitz DE, Ryoo S. Arginase II activity regulates cytosolic Ca(2+) level in a p32-dependent manner that contributes to Ca(2+)-dependent vasoconstriction in native low-density lipoprotein-stimulated vascular smooth muscle cells. *Exp Mol Med* 2019;**51**:1–12. [CVOCROSSCVO]

Translational perspective

In many vascular disorders, the downregulation of arginase II (ArgII) has been shown to be beneficial. This enzyme plays a crucial role in the regulation Ca^{2+} concentrations in a p32-dependent manner and activates the endothelial nitric oxide synthase activation signalling cascade. In this study, we discovered that ArgII downregulation, inhibition of its activity, and gene knockout/down, induced the activation of Parkin (an E3-ubiquitin ligase) through a CaMKII-dependent mechanism. ArgII protein, as a p32 binding partner, prevented Parkin-dependent p32 ubiquitination, but inhibition of ArgII activity had no effect on ubiquitination. These novel findings have the potential to be translated into future therapeutic strategies to treat vascular diseases.